THE GEOLOGICAL SOCIETY OF AMERICA®

Accelerating slip rates on the Puente Hills blind thrust fault system beneath metropolitan Los Angeles, California, USA

Kristian J. Bergen[1], John H. Shaw[1*], Lorraine A. Leon[2†], James F. Dolan[2], Thomas L. Pratt[3], Daniel J. Ponti[4], Eric Morrow[1], Wendy Barrera[5], Edward J. Rhodes[5,6], Madhav K. Murari[7], and Lewis A. Owen[7]

[1]Department of Earth and Planetary Sciences, Harvard University, Cambridge, Massachusetts 02138, USA
[2]Department of Earth Sciences, University of Southern California, Los Angeles, California 90089, USA
[3]U.S. Geological Survey, Reston, Virginia 20192, USA
[4]U.S. Geological Survey, Menlo Park, California, USA
[5]Department of Earth, Planetary and Space Sciences, University of California, Los Angeles, California 90095, USA
[6]Department of Geography, University of Sheffield, Sheffield S10 2TN, UK
[7]Department of Geology, University of Cincinnati, Cincinnati, Ohio 45221, USA

ABSTRACT

Slip rates represent the average displacement across a fault over time and are essential to estimating earthquake recurrence for probabilistic seismic hazard assessments. We demonstrate that the slip rate on the western segment of the Puente Hills blind thrust fault system, which is beneath downtown Los Angeles, California (USA), has accelerated from ~0.22 mm/yr in the late Pleistocene to ~1.33 mm/yr in the Holocene. Our analysis is based on syntectonic strata derived from the Los Angeles River, which has continuously buried a fold scarp above the blind thrust. Slip on the fault beneath our field site began during the late-middle Pleistocene and progressively increased into the Holocene. This increase in rate implies that the magnitudes and/or the frequency of earthquakes on this fault segment have increased over time. This challenges the characteristic earthquake model and presents an evolving and potentially increasing seismic hazard to metropolitan Los Angeles.

INTRODUCTION

The Puente Hills blind thrust fault system (PHT) extends for 40 km across the Los Angeles basin (California, USA) and presents one of the largest deterministic seismic risks in the United States (Shaw and Shearer, 1999; Dolan et al., 2003; Field et al., 2005) (Fig. 1A). Blind thrusts do not reach the Earth's surface, complicating assessment of their activity and slip rate. Their surface expression, if any, is often as folds (e.g., Stein and Yeats, 1989; Shaw and Suppe, 1996; Shaw and Shearer, 1999; Champion et al., 2001). The M_w 6.7 Northridge earthquake demonstrated the damaging effects of blind thrust earthquakes, causing 60 fatalities and an estimated \$13–\$40 billion in damage to the Los Angeles region (National Oceanic and Atmospheric Administration National Centers for Environmental Information, 1994). The PHT presents a greater potential hazard due to its size and proximity to the most populated regions of Los Angeles (Field et al., 2005).

The motivation of our research is to determine a contemporary slip rate on the Los Angeles segment of the PHT, which underlies downtown Los Angeles. Our site also provides the opportunity to investigate the continuity of slip rates over the past 500 k.y., thanks to the continual burial of fold scarps by sediment from the Los Angeles River. In contrast, most geologic assessments of slip rates rely on paleoseismology methods that sample only the last few tens of thousands of years (e.g., Dolan et al., 2003), or geologic cross sections that define slip rates over millions of years (e.g., Huftile and Yeats, 1995). The intervening several hundred thousand year time span is rarely constrained, yet this period has important implications for long-standing questions about the characteristic earthquake model (e.g., Jacoby et al., 1988; Kagan et al., 2012) and temporal earthquake clustering (e.g., Grant and Sieh, 1994; Dolan et al., 2007), as changes in slip rate over time imply changes in earthquake magnitudes, frequency, and/or slip distributions. The implications for probabilistic seismic hazard assessments are perhaps greater, as changes in slip rate would complicate estimates of earthquake recurrence (Youngs and Coppersmith, 1985).

GEOLOGICAL AND SEISMOLOGICAL SETTING

The PHT is within the Los Angeles basin, which contains a thick succession of Quaternary through Cretaceous sedimentary units above Mesozoic basement (Wright, 1991). The PHT was identified as the source of the 1987 M_w 6.0 Whittier Narrows earthquake (Shaw and Shearer, 1999) and includes three main segments, the Coyote Hills, Santa Fe Springs, and Los Angeles (Fig. 1A). The tips of these faults are overlain by a series of east-west–trending, en echelon anticlines (Shaw et al., 2002; Leon et al., 2007). Using earthquake magnitude-scaling relationships for thrust faults (Wells and Coppersmith, 1994), it was estimated (Shaw and Shearer, 1999) that the PHT could generate M_w 6.5–6.6 and M_w 7.1 earthquakes for single and multisegment rupture scenarios, respectively. Slip-event data, however, suggest potentially larger magnitudes of M_w 7.2–7.5 for multisegment ruptures (Dolan et al., 2003).

The southern margins of the anticlines above the PHT have narrow forelimbs that are pinned at depth to the upper tiplines of the blind fault ramps (Pratt et al., 2002; Shaw et al., 2002). Pliocene and younger strata thin across the folds, indicating that these units represent growth (syntectonic) stratigraphy (Suppe et al., 1992; Shaw and Suppe, 1994). These growth strata are flood deposits from the Los Angeles and San Gabriel Rivers that continually buried the fold scarps, recording the amount of relative uplift as the difference in stratigraphic thickness between the uplifted fold crest and the adjacent footwall trough. Based on these differences, average slip rates over the past 1.6 m.y. have been estimated to be 0.44–1.7 mm/yr across all three segments (Shaw et al., 2002). Subsequent work refined the Holocene slip rate on the Santa Fe Springs segment to ≥0.9–1.6 mm/yr (Dolan et al., 2003; Leon et al., 2007).

DATA AND METHODS

We estimate slip rates on the Los Angeles segment using seismic reflection data and a range of dating methods. Industry seismic reflection data image a fold limb with growth stratigraphy above the Los Angeles

*E-mail: shaw@eps.harvard.edu
†Current address: Chevron North America Exploration and Production, Bakersfield, California 93311, USA.

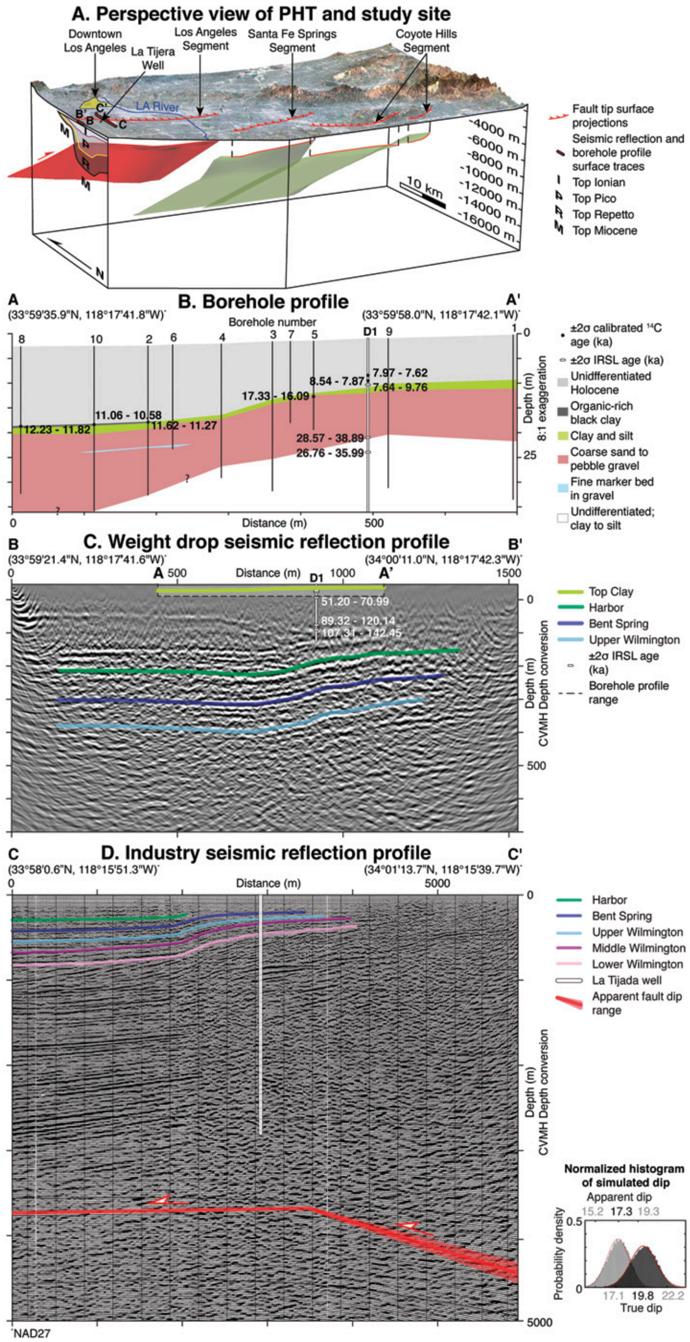

Figure 1. A: Perspective view of the Puente Hills blind thrust fault system (PHT; California, USA) from the Southern California Earthquake Center (SCEC) Community Fault Model (Plesch et al., 2007), highlighting the Los Angeles segment in red. The locations of the seismic reflection profiles B-B′ and C-C′ in C and D are indicated. The borehole profile A-A′ is within B-B′. Surface topography is vertically exaggerated (5:1); other dimensions are 1:1. LA—Los Angeles. B: Shallow borehole profile. Boreholes 1–10 are continuously cored hollow-stem auger boreholes. Borehole D1 was drilled with both hollow-stem auger and mud-rotary techniques to sample a greater depth range. To produce the vertical relief observed across the clay and silt unit (green) given the estimated fault dips (see D), a total of 17.75–22.72 m slip is required (2.5–97.5 percentile ranges). This indicates the occurrence of several earthquakes between deposition of the clay and silt layer and the overlying organic-rich black clay that buttresses the fold. The geometry of the top clay and ^{14}C ages from wells 8 and 5 were used for our most recent slip rate estimates. IRSL—infrared stimulated luminescence. C: Weight drop seismic reflection profile, depth-converted using the SCEC Community Velocity Model-Harvard (CVMH; with geotechnical layer; https://scec.usc.edu/scecpedia/CVM-H) (Shaw et al., 2015). D: Industry seismic reflection profile showing the broader Los Angeles segment fold structure. The apparent fault dip range in red encompasses the 2.5–97.5 percentile range from our simulations, as shown in the adjacent histogram.

segment (Fig. 1D). High-frequency seismic reflection data (Fig. 1C), a series of continuously cored hollow-stem auger boreholes (Fig. 1B), and a deeper (175 m) mud-rotary borehole (Figs. 1B and 1C) were acquired for this study to constrain the shallow geometry of the fold and determine the most recent fault activity. To provide Pleistocene stratigraphic markers, sequence boundaries from the Ponti et al. (2007) Long Beach area framework were mapped to our high-frequency seismic reflection profiles (20–25 km away) using additional well logs and our industry seismic reflection data. Lithological correlations from the boreholes were used to map the fold geometry into the Holocene. Age constraints were provided by marine oxygen isotope stages (MIS) for the sequence boundaries (Ponti et al., 2007; McDougall et al., 2012). For the borehole lithological correlations we used radiocarbon (^{14}C) and single-grain K-feldspar post-IR IRSL (infrared stimulated luminescence) dating (Rhodes, 2015; see results and technical details in the GSA Data Repository[1]). The fold geometry is consistent with growth stratigraphy deposited above the forelimb of a fault-bend fold (Suppe et al., 1992; Shaw and Shearer, 1999; Pratt et al., 2002) (Fig. 1C; Fig. DR1 in the Data Repository); we used this insight to model the underlying fault geometry and relate uplift to fault slip as described in the Data Repository.

We adopt a probabilistic approach that accounts for uncertainties in both ages and stratigraphic geometries to estimate slip rate probability density functions over a series of time intervals. We developed an autoregressive statistical model (AR) of interval velocities from the nearby La Tijera industry well (Figs. 1A and 1D) to simulate velocity models for depth conversion of our high-frequency seismic reflection data. To account for resolution uncertainties, we randomly repositioned the interpreted sequence boundaries within an estimated one-half wavelength resolution limit of the seismic data (Vail et al., 1977). To account for any thickness changes due to differential compaction across the fold, we used exponential porosity-depth relations (Athy, 1930) to estimate depositional thicknesses. Bed dip and sediment thickness changes across the fold were then calculated for each simulation and used to determine fault geometry and slip. Probability distributions for our age determinations were sampled at random and combined with our slip estimates to calculate slip rate probability distributions.

Figure 2 shows the estimated distributions for fold crest depth, trough depth, and structural relief along with associated age distributions. Slip rate distributions are shown in Figure 3 and in Table DR1d. These are geometrically related to the vertical relief in Figure 2 by corresponding fault dips, shown in Figure 1D and in Table DR1e. Sedimentation rates based on trough position and age (dark blue in Fig. 2) are shown in Figure DR9 and Table DR1a. Horizontal shortening and uplift rate distributions are shown in Figure DR10 and Table DR1d.

DISCUSSION

The most recent time period defined by our study is from the top clay horizon (17.6–11.7 ka) to the present. The total slip over this period ranges from 17.75 to 22.72 m (2.5–97.5 percentile ranges), confirming the occurrence of multiple earthquakes to support our slip rate estimate in this period of 1.13–1.73 mm/yr (2.5–97.5 percentile ranges). This range is consistent with Holocene slip rates of ≥0.9–1.6 mm/yr obtained on the

[1]GSA Data Repository item 2017059, detailed description of the datasets and methods used to calculate fault slip rates, including an assessment of uncertainties, is available online at www.geosociety.org/datarepository/2017 or on request from editing@geosociety.org. In addition, seismic reflection data acquired for this study are archived at: https://www.sciencebase.gov/catalog/item/582c9a58e4b04d580bd3786d.

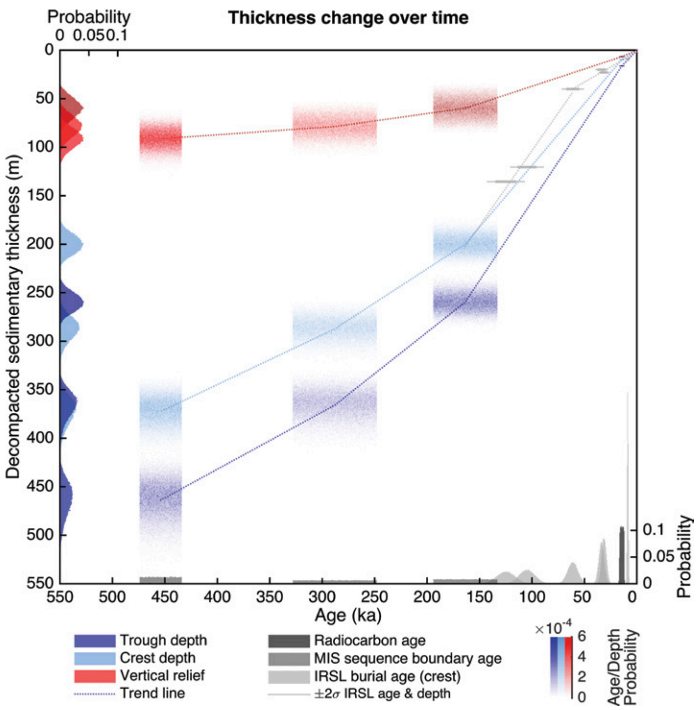

Figure 2. Thickness and vertical relief change over time. Normalized probability distributions of crest, trough, and vertical relief values from our simulations are shown along the y axis (1 m bins). Sampled age distributions for the sequence boundaries, top clay, and infrared stimulated luminescence (IRSL) samples are shown on the x axis (500 yr bins). MIS—marine oxygen isotope stage. Bivariate age/depth histograms from our simulations are shown with color intensity scaled to probability. Bin widths correspond to the depth and age bins. Trend lines through the mean values are shown, with least squares fitted trend lines for the IRSL data.

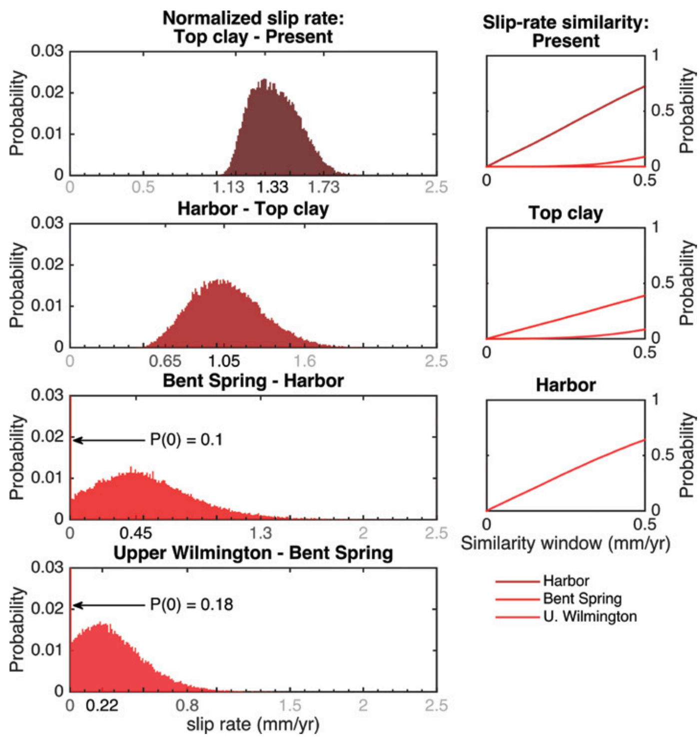

Figure 3. Probability normalized histograms of slip rates with 2.5–97.5 percentile ranges shown between the stratigraphic boundaries given in the figure titles. Median values are shown for symmetric distributions and modal values for skewed distributions. Bin size is 0.1 mm/yr. The slip rate similarity plots show the probability of producing fold geometries with similar slip rates from the ages of the boundaries listed in the title across prior intervals, given the uncertainties in our data. The similarity window is the absolute difference in slip rate within which values are considered similar. U.—Upper.

central Santa Fe Springs segment of the PHT (Dolan et al., 2003; Leon et al., 2007), supporting the view that these two segments behave as a linked system. Comparison of horizontal shortening rates from the top clay to the present of 1.06–1.63 mm/yr (2.5–97.5 percentile range; Table DR1d) to geodetically determined shortening estimates across the Los Angeles region of 4.4 ± 0.8 mm/yr from Bawden et al. (2001) and 4.5 ± 1 mm/yr from Argus et al. (2005) suggests that the Los Angeles segment may account for about one-third of the modern shortening across the basin.

Examining the slip rate data from earlier time intervals, significant motion on the Los Angeles segment at our site began between creation of the Bent Spring and the Harbor sequence boundaries during the late-middle Pleistocene and progressively increased through the late Quaternary (Fig. 3). This is demonstrated in the slip rate similarity plots in Figure 3, which show the probability that slip rate remains constant across previous time intervals, given the uncertainties in our data. We assessed if slip rates were similar by calculating the difference between them across all time intervals for each individual model iteration, in a stepwise fashion from the present backward in time. Only values meeting the similarity criterion (i.e., could have similar slip rates between time steps) in more recent time intervals were considered for similarity in subsequent steps. To the present day, ~36% of our simulations had slip rates within 0.25 mm/yr of each other over the 2 time intervals following creation of the Harbor sequence boundary. Of these, however, none met the 0.25 mm/yr criterion across prior intervals. Increasing the similarity window to 0.5 mm/yr, 9% of our simulations survived to the Bent Spring sequence boundary, and 4 out of 50,000 simulations (8×10^{-5}) satisfied these conditions back to creation of the Upper Wilmington sequence boundary. This demonstrates that the slip rate on the Los Angeles segment has almost certainly accelerated since formation of the Bent Spring sequence boundary, and that it likely continued to increase after formation of the Harbor sequence boundary to the present day. This accelerating pattern highlights the importance of using slip rates averaged over recent time periods for probabilistic seismic hazard assessments. Our results, for example, show that PHT slip rates determined from older strata, and thus averaged over longer time intervals, yield lower estimates of earthquake recurrence than indicated by our most recent slip rates.

We propose three reasons for the observed accelerating slip rate at our site: the frequency of earthquakes could have increased, the average displacement per earthquake could have increased, or both. Given our location at the western margin of the Los Angeles segment, we suggest that the most likely explanation is that displacement per earthquake has increased at our study site as the fault tip has propagated laterally to the west. Such behavior has been documented for other blind thrusts (Grothe et al., 2014), and seems plausible here given the location of our site. This implies that the Los Angeles segment has grown laterally over the late Quaternary, and that its maximum potential earthquake magnitude and seismic hazard may have correspondingly increased. While research on displacement-length relationships for thrust faults is limited, it is generally found that longer fault lengths correspond to greater displacements, supporting our view that lateral fault-tip propagation could increase earthquake magnitude (e.g., Bergen and Shaw, 2010). If this is the case, it directly challenges the characteristic earthquake model assumption of regular, repeating rupture patterns (i.e., rupture size and displacement) on individual fault segments over many earthquake cycles (Grant, 1996). If earthquakes were occurring more frequently instead, or in addition to growing in magnitude, this would imply an increase in loading rates that would also raise the seismic hazard on the Los Angeles segment of the PHT.

Our interpretation also has regional implications. As slip rates on the Los Angeles segment are increasing, it implies that either slip is being transferred to the PHT from another fault system that would have decreasing slip through time (redistributing a constant total hazard to different parts of the basin), or the total shortening rate across the Los Angeles basin has increased with time (increasing hazard throughout the basin). In the latter scenario, the PHT could be accommodating all of the increase, or slip rates on multiple fault systems could have increased. These scenarios point to evolution of both the PHT fault system and the regional tectonics, adding complexity to, and likely increasing, the seismic hazard to metropolitan Los Angeles.

ACKNOWLEDGMENTS

We thank the National Science Foundation (NSF) EAR RAPID (Division of Earth Sciences, Rapid Response Research) and Tectonics programs, which facilitated drilling and data collection in a narrow time frame when the site remained accessible (NSF grants EAR-0946261, EAR-0920947, EAR-0711170, and EAR-0711220). We also acknowledge the Southern California Earthquake Center for supporting early studies of the Puente Hills blind thrust fault system that laid the groundwork for this investigation, and the U.S. Geological Survey Earthquake Hazards Program for contributions to this effort. We also thank the numerous field assistants that helped us acquire data for this study, and Carling Hay and Erik Chan for their helpful discussions. We are also indebted to the reviewers (Karl Mueller, Christopher Jackson, Christopher Sorlien, and Kate Scharer) for their helpful comments. Any use of trade, firm, or product names is for descriptive purposes only and does not imply endorsement by the U.S. Government.

REFERENCES CITED

Argus, D.F., Heflin, M.B., Peltzer, G., Webb, F.H., and Crampe, F., 2005, Interseismic strain accumulation and anthropogenic motion in metropolitan Los Angeles: Journal of Geophysical Research, v. 101, B04401, p. 2156–2202, doi:10.1029/2003JB002934.

Athy, L.F., 1930, Density, porosity, and compaction of sedimentary rocks: American Association of Petroleum Geologists Bulletin, v. 14, p. 1–24.

Bawden, G., Thatcher, W., Stein, R.S., Hudnut, K., and Peltzer, G., 2001, Tectonic contraction across Los Angeles after removal of groundwater pumping effects: Nature, v. 412, p. 812–815, doi:10.1038/35090558.

Bergen, K.J., and Shaw, J.H., 2010, Displacement profiles and displacement-length scaling relationships of thrust faults constrained by seismic-reflection data: Geological Society of America Bulletin, v. 122, p. 1209–1219, doi:10.1130/B26373.1.

Champion, J., Mueller, K., Tate, A., and Guccione, M., 2001, Geometry, numerical models and revised slip rate for the Reelfoot fault and trishear fault-propagation fold, New Madrid seismic zone: Engineering Geology, v. 62, p. 31–49, doi:10.1016/S0013-7952(01)00048-5.

Dolan, J.F., Christofferson, S.A., and Shaw, J.H., 2003, Recognition of paleoearthquakes on the Puente Hills blind thrust fault, California: Science, v. 300, p. 115–118, doi:10.1126/science.1080593.

Dolan, J.F., Bowman, D.D., and Sammis, C.G., 2007, Long-range and long-term fault interactions in southern California: Geology, v. 35, p. 855–858, doi:10.1130/G23789A.1.

Field, E.H., Seligson, H.A., Gupta, N., Gupta, V., Jordan, T.H., and Campbell, K.W., 2005, Loss estimates for a Puente Hills blind-thrust earthquake in Los Angeles, California: Earthquake Spectra, v. 21, p. 329–338, doi:10.1193/1.1898332.

Grant, L.B., 1996, Uncharacteristic earthquakes on the San Andreas fault: Science, v. 272, p. 826–827, doi:10.1126/science.272.5263.826.

Grant, L.B., and Sieh, K.E., 1994, Paleoseismic evidence of clustered earthquakes on the San Andreas fault in the Carrizo Plain, California: Journal of Geophysical Research, v. 99, p. 6819–6841, doi:10.1029/94JB00125.

Grothe, P.R., Cardozo, N., Mueller, K., and Ishiyama, T., 2014, Propagation history of the Osaka-wan blind thrust, Japan, from trishear modeling: Journal of Structural Geology, v. 58, p. 79–94, doi:10.1016/j.jsg.2013.10.014.

Huftile, G.J., and Yeats, R.S., 1995, Convergence rates across a displacement transfer zone in the Western Transverse Ranges, Ventura basin, California: Journal of Geophysical Research, v. 100, p. 2043–2067, doi:10.1029/94JB02473.

Jacoby, G.C., Sheppard, P.R., and Sieh, K.E., 1988, Irregular recurrence of large earthquakes along the San Andreas fault—Evidence from trees: Science, v. 241, p. 196–199, doi:10.1126/science.241.4862.196.

Kagan, Y.Y., Jackson, D.D., and Geller, R.J., 2012, Characteristic earthquake model, 1884–2011, RIP: Seismological Research Letters, v. 83, p. 951–953, doi:10.1785/0220120107.

Leon, L.A., Christofferson, S.A., Dolan, J.F., Shaw, J.H., and Pratt, T.L., 2007, Earthquake-by-earthquake fold growth above the Puente Hills blind thrust fault, Los Angeles, California: Implications for fold kinematics and seismic hazard: Journal of Geophysical Research, v. 112, B03S03, p. 2156–2202, doi.10.1029/2006JB004461.

McDougall, K., Hillhouse, J., Powell, C.I.I., Mahan, S., Wan, E., and Sarna-Wojcicki, A.M., 2012, Paleontology and geochronology of the Long Beach core sites and monitoring wells, Long Beach, California: U.S. Geological Survey Open-File Report 2011-1274, 235 p.

National Oceanic and Atmospheric Administration National Centers for Environmental Information, 1994, Significant earthquake: California, Northridge: http://www.ngdc.noaa.gov/nndc/struts/results?eq_0=5372&t=101650&s=13&d=22,26,13,12&nd=display (January 2014).

Plesch, A., et al., 2007, Community fault model (CFM) for southern California: Seismological Society of America Bulletin, v. 97, p. 1793–1802, doi:10.1785/0120050211.

Ponti, D.J., et al., 2007, A 3-dimensional model of water-bearing sequences in the Dominguez Gap region, Long Beach, California: U.S. Geological Survey Open-File Report 2007-1013, 34 p.

Pratt, T.L., Shaw, J.H., Dolan, J.F., Christofferson, S., Williams, R.A., Odum, J.K., and Plesch, A., 2002, Shallow seismic imaging of folds above the Puente Hills blind-thrust fault, Los Angeles, California: Geophysical Research Letters, v. 29, p. 18-1–18-4, doi:10.1029/2001GL014313.

Rhodes, E.J., 2015, Dating sediments using potassium feldspar single-grain IRSL: initial methodological considerations: Quaternary International, v. 362, p. 14–22, doi:10.1016/j.quaint.2014.12.012.

Shaw, J.H., and Shearer, P.M., 1999, An elusive blind-thrust fault beneath metropolitan Los Angeles: Science, v. 283, p. 1516–1518, doi:10.1126/science.283.5407.1516.

Shaw, J., and Suppe, J., 1994, Active faulting and growth folding in the eastern Santa Barbara Channel, California: Geological Society of America Bulletin, v. 106, p. 607–626, doi:10.1130/0016-7606(1994)106<0607:AFAGFI>2.3.CO;2.

Shaw, J.H., and Suppe, J., 1996, Earthquake hazards of active blind-thrust faults under the central Los Angeles basin, California: Journal of Geophysical Research, v. 101, p. 8623–8642, doi:10.1029/95JB03453.

Shaw, J.H., Plesch, A., Dolan, J.F., Pratt, T.L., and Fiore, P., 2002, Puente Hills blind-thrust system, Los Angeles, California: Seismological Society of America Bulletin, v. 92, p. 2946–2960, doi:10.1785/0120010291.

Shaw, J.H., et al., 2015, Unified structural representation of the southern California crust and upper mantle: Earth and Planetary Science Letters, v. 415, p. 1–15, doi:10.1016/j.epsl.2015.01.016.

Stein, R.S., and Yeats, R.S., 1989, Hidden earthquakes: Scientific American, v. 260, p. 48–57, doi:10.1038/scientificamerican0689-48.

Suppe, J., Chou, G., and Hook, S., 1992, Rates of folding and faulting determined from growth strata, *in* McClay, K., ed., Thrust tectonics: London, Chapman Hall, p. 105–121, doi:10.1007/978-94-011-3066-0_9.

Vail, P.R., Todd, R.G., and Sangree, J.B., 1977, Seismic stratigraphy and global changes of sea level: Part 5. Chronostratigraphic significance of seismic reflections, *in* Payton, C.E., ed., Seismic stratigraphy—Applications to hydrocarbon exploration: American Association of Petroleum Geologists Memoir 26, p. 99–116, doi:10.1306/M26490C7.

Wells, D.L., and Coppersmith, K.J., 1994, New empirical relationships among magnitude, rupture length, rupture width, rupture area, and surface displacement: Seismological Society of America Bulletin, v. 84, p. 974–1002.

Wright, T.L., 1991, Structural geology and tectonic evolution of the Los Angeles Basin, California, *in* Biddle, K., ed., Active margin basins: American Association of Petroleum Geologists Memoir 52, p. 35–134.

Youngs, R.R., and Coppersmith, K.J., 1985, Implications of fault slip rates and earthquake recurrence models to probabilistic seismic hazard estimates: Seismological Society of America Bulletin, v. 75, p. 939–964.

Manuscript received 24 August 2016
Revised manuscript received 17 November 2016
Manuscript accepted 21 November 2016

Printed in USA